Production and Characterization of CNC Reinforced Polyamide-6 Nano-Composite Films

E.C. Demir[1], A. Benkaddour[1,2], N. Jankovic[2], M.T. McDermott[2], C.I. Kim[1], C. Ayranci[1]*
[1] Department of Mechanical Eng., University of Alberta, Edmonton, Alberta, Canada
[2] Department of Chemistry, University of Alberta, Edmonton, Alberta, Canada
* Corresponding author (cayranci@ualberta.ca)

ABSTRACT

Cellulose nanocrystals (CNC) are novel bio-based nano-fibers. Their high aspect and surface-to-volume ratios, low density, and attractive mechanical properties make them ideal candidates as a reinforcement for nanocomposites. Polyamide 6 (PA6) is one of the most commonly used thermoplastics in the world; however, the potential for CNC reinforcement of PA6 has not been fully explored. This paper reports on CNC reinforced PA6 films produced by solvent mixing in formic acid and processed using spin coating. PA6 was reinforced with different level of CNC. The work outlines use of DSC and XRD techniques to explore relationships between mechanical properties and crystallinity of the composites in addition to CNC effect on crystallography of PA6. Samples were subjected to uniaxial tension test at room temperature with C-shaped mechanical support to prevent sliding of films or stress concentration, which can be due to clamps. Experiments show promising increase in elastic modulus and strength compared to non-reinforced samples.

KEYWORDS: Cellulose nanocrystals, PA6, Nanocomposite

1 INTRODUCTION

Polymeric materials are the basis of many products worldwide. While many applications can be satisfied using pure polymers, others require the polymer to exhibit improved and/or controllable properties. Properties such as mechanical strength, conductivity and thermal response can be improved by the addition of micron- and nano-sized materials to the polymer matrix. In terms of mechanical properties, there has been large amount of work done to reinforce polymers with different types, sizes and shapes of materials (Nilagiri Balasubramanian & Ramesh, 2018; Peitl, Oréfice, Hench, & Brennan, 2004; Shen, Fang, Chen, & Tang, 2011; Shishkovsky, Sherbakov, Ibatullin, Volchkov, & Volova, 2018). The field of polymeric nanocomposite development has gained significant momentum due to the promise of producing materials with unique and tailorable mechanical, physical, and chemical properties (Kuilla et al., 2010; Lebaron, Wang, & Pinnavaia, 1999; Paul & Robeson, 2008).

Cellulose is the world's most abundant biopolymer and has been utilized in countless applications for many years. Nanomaterials extracted from cellulose have become a main focus of both academic and industrial research as reinforcing agents for polymers. Cellulose nanocrystals (CNC) can be extracted from variety of sources such as Kenaf, Cotton (Dufresne, A., 2012) . As the name implies, CNC are crystalline, rod-shaped nanoparticles with excellent properties for reinforcement. These include high aspect and surface to volume ratio (150-600 m^2g^{-1}), high Young's modulus (100-150 GPa) and low density (1.5-1.6 gcm^{-3}). These properties have drawn significant attention and make them perfect candidate for nano-composite development (Dufresne, Alain, 2013).

Polyamide 6 (PA6) is one of the most used engineering thermoplastics. Although there have been efforts to reinforce it with nanoparticles, such as clay, (Kojima et al., 1993; Lebaron, Wang, & Pinnavaia, 1999; Liu, Qi, & Zhu, 1999), there is limited amount of study on CNC reinforced PA6 with the exception of few (Kashani Rahimi & Otaigbe, 2016; Qua & Hornsby, 2011; Yousefian & Rodrigue, 2017) which are based on melt mixing process. Consequently, in this study, solution based spin coating process is used to produce CNC reinforced PA6 nanocomposites that has been never covered in the literature.s

2 MATERIALS AND METHODOLOGY

PA6 (25038-54-4) and Formic acid (FA, 98%) were purchased from Sigma Aldrich and used as received. CNC were obtained from InnoTech Alberta (Edmonton, AB, Canada). The CNC was produced by sulphuric acid hydrolysis of bleached softwood Kraft pulp.

CNC/PA6 nanocomposite films were prepared by solvent mixing in formic acid and spin coating. A rectangular shaped (25mm × 75mm) glass substrate was coated with 2 ml of suspension before spinning. The substrate rotational speed was brought to 2000 rpm for 15 seconds and then 3000 rpm for 30 seconds. After spinning the substrate allowed to rest for 5 minutes so that any remaining solvent can evaporate. As a result, 1.0, 2.5 and 5.0 wt% CNC reinforced films were produced with 10-15 µm thicknesses.

PA6 is a semi-crystalline polymer and its structure is expected to change as CNC is added. Assessment of the crystallinity was accomplished using differential scanning calorimetry (DSC) and X-ray diffraction (XRD). Uniaxial tension tests were performed to determine mechanical properties of the films. In this paper all CNC loading percentages refer to weight percentage.

2.1 Differential Scanning Calorimetry

Films were cut to obtain 5 mg samples to perform thermal analysis. One sample was tested from each CNC loading level. Samples were encapsulated with hermetic aluminium DSC pans. Thermal analysis was performed with TA Instrument DSC Q2000. Samples were heated from 25°C to 300°C with 20°C/min rate. Crystallinity of the polymer was calculated using Eqn. (1):

$$\%Crystallinty = \frac{\Delta H_m - \Delta H_c}{w_f * \Delta H_r}\, x\, 100 \qquad (1)$$

Where ΔH_m is area under melting peak, ΔH_c area under cold crystallization peak, ΔH_r enthalpy required to melt the polymer (J/g), w_f is the weight fraction matrix.

2.2 X-Ray Diffraction

Rigaku XRD ultima IV was used for XRD analysis. Spin coated samples were not peeled off from glass substrate to keep them flat. While angle of arm which sends Cu K-α radiation is kept constant to prevent possible diffractions which may come from glass, collector arm is rotated such that data is collected from 10° to 35° with 1°/min rate. One sample was tested for each level of CNC loading.

2.3 Uniaxial Tension Tests

TA instrument ElectroForce 3200 with 10 N load cell was used to assign mechanical properties of the films. Films, Figure 1 (a), were cut into (10mmx75mm) size from the middle of the glass substrate after each spinning process to prevent any edge effect which may arise from the spinning process. Rotary cutter and 3D printed custom cutting plate were utilized for sample size consistency. Samples were stored overnight in a desiccator containing silica gel before testing. Distance between grips was adjusted to 50 mm and grips hold 25 mm of the sample. Since samples were between 10-15 µm and smooth, C shaped paper was used as a mechanical support to prevent sliding and reduce stress concentration which may come from grips. Paper was inserted between the grips and sample, then it was cut from the middle after clamps

hold the sample as shown in Figure 1 (b). The clamps of the tester were tightened with 4-in.lb torque. Samples were loaded with 0.083 mm/sec (0.1 mm.mm/min).

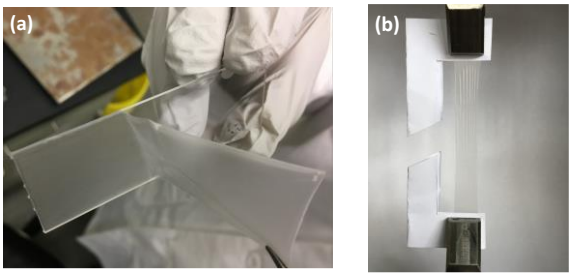

Figure 1. Photos of sample; while peeling off from glass substrate (a) and under tensile test with C shaped mechanical support (b).

3 RESULTS AND DISCUSSION

The mechanical response of a material is directly related to its structure (Habr, Seidl, & Bobek, 2016; Panthani & Bates, 2015; Ye et al., 2017). PA6 is a semi-crystalline thermoplastic, having both amorphous and crystalline regions and it is expected that the addition of CNC will alter the structure. Thus our efforts here are focused on correlating the crystalline structure of the CNC/PA6 nanocomposites with the mechanical properties. We used both XRD and DSC to probe the structure of the CNC/PA6 films as a function of loading. Figure 2 (a) contains the XRD pattern for pure PA6 and PA6 with various CNC loadings. Characteristic diffractions peaks of PA6 are expected between 10-35° according to literature (Millot, Fillot, Lame, Sotta, & Seguela, 2015; Weng, Chen, & Wu, 2003). The XRD pattern exhibits peaks corresponding to two main crystal phases α-crystal and γ-form. It is observed from the XRD pattern that intensities and width of peaks are altered as CNC content changes. The pure PA6 films yield peaks for both crystal forms. For samples reinforced with 1.0% and 2.5% CNC, the α_1 peaks become more apparent. The intensity of the γ peak at $2\theta \approx 21.6°$ decreases for these loading levels but increases for the 5.0% CNC/PA6 sample. According to (Murthy, Aharoni, & Szollosi, 1985), γ is a meta-stable phase which is usually formed when there is a high cooling rate in the solidification process and more amorphous structure is formed. Annealing at high temperature induces a phase change in PA6 from γ to α crystals. Both of these can exist depending on the process (Murthy et al., 1985). A second peak of γ at $2\theta \approx 10.5°$ is also visible for 5.0% CNC/PA6. It is obvious that γ is formed for pure PA6 and 5.0% CNC/PA6 composite. Spin coating is a relatively rapid process for the crystallization of PA6 and thus both the γ form and the α phase along with amorphous regions are all present. The γ form is dominant over the α in pure PA6. The CNC at lower loadings (1 and 2.5%) are sufficiently well-dispersed that they act as nucleation sites for α phase crystallization. However, it is likely that the CNC is more aggregated at 5.0% loading which results in a decrease in α_1 intensity and increase in the γ peaks. The DCS analysis for the films is shown in Figure 2 (b). Cold crystallization is usually observed for semi-crystalline polymer however PA6 films did not show clear exothermic cold crystallization peak which occurs due to crystallization of amorphous portion of the polymer. In literature, (Fornes & Paul, 2003; Millot et al., 2015), PA6 exhibits similar thermal behaviours except for quenched PA6. When PA6 is quenched, amorphous region is expected to be more in terms of both quantity and disorders of molecules. Therefore, only the area under the melting region is calculated using TA Universal 2000 software to ascertain crystallinity percentage. Heat of fusion to melt the 100% PA6 (ΔH_r) was taken 230 J/g according (Wunderlich, 1990) and it was assumed that heat of fusion is independent of temperature. Crystallinity percent of composites are given in Table 1.

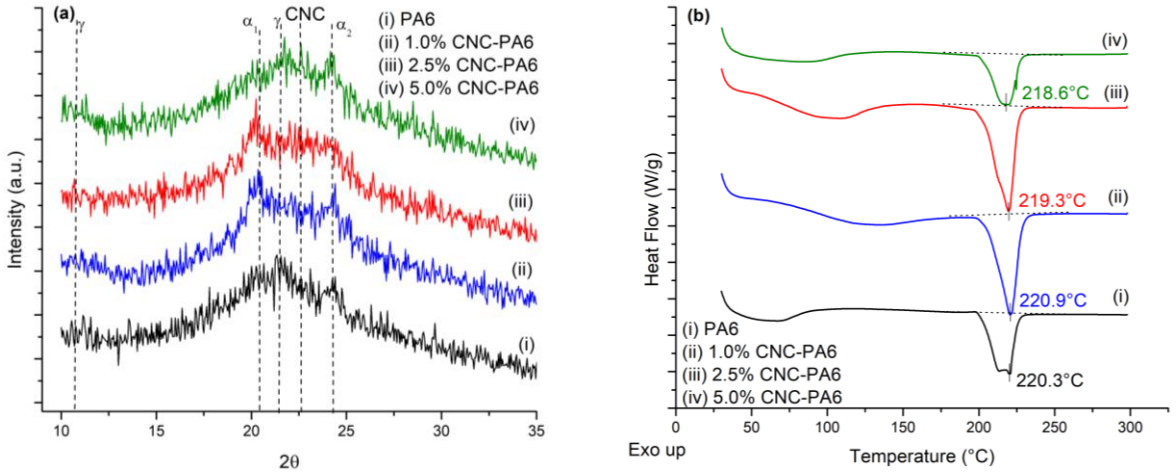

Figure 2. XRD patterns (a) and DSC graphs (b) of PA6 with different CNC loadings.

Table 1. Crystallinity percentage of PA6 according to area under curve of DSC graphs given in .

Composite	**PA6**	**1.0% CNC-PA6**	**2.5% CNC-PA6**	**5.0% CNC-PA6**
% Crystallinity	25.9	24.6	32.6	24.6

When XRD and DSC results are considered, it is observed that the crystallinity percent first increases but then decreases as CNC loading is increased to 1.0% and 5.0% from pure PA6. Although CNC helps forming of α phase and increase in crystallinity of PA6, results indicate that after a point it loses its effect potentially due to agglomeration size and distribution. If the spinning rate is decreased and CNC is added at different levels, change in both crystallinity percent and crystalline type are expected.

PA6 is one of the most commonly utilized engineering polymers which requires high elastic modulus and tensile strength. Elastic modulus of the samples was calculated as slope from the region where second slope of the stress strain curve is zero. Tensile strength was recorded as maximum stress in the stress-strain curve. Figure demonstrates elastic modulus (a) and tensile strength (b) average values out of at least 3 samples with different CNC loading levels.

Analysis of stress-strain curve and results given as a bar chart in Figure , proves that CNC reinforces PA6. Maximum enhancement, compared to un-reinforced PA6, in elastic modulus and tensile strength is 48% and 54% respectively at 5.0% CNC addition. Dispersion of CNC in PA6 and interaction between CNC and PA6 are expected to be high since both of them are polar materials. While CNC has OH groups on its surface, PA6 has amide groups. It is expected to have hydrogen bonding between CNC and PA6. When 0, 2.5% and 5.0% is examined, there is clear increase in mechanical properties. However, in the case of 1.0% CNC, there is a jump compared to others which can be proposed because of good dispersion. Specially in nanocomposite, nanoparticles tend to agglomerate. These agglomerated particles can behave as a stress concentration point and instead of carrying load, they would be the reason of failure beginning. Decrease in the increase of elastic modulus and tensile strength can be explained with imperfections in the structure. 1.0% CNC is assumed to have best distribution so it has high elastic modulus with high tensile strength. Agglomeration may start at 2.5% CNC however it is not as high as 5.0% CNC because it should be thought that if all particles were agglomerated, matrix would behave as almost pure material and could not show any peaks of α phase.

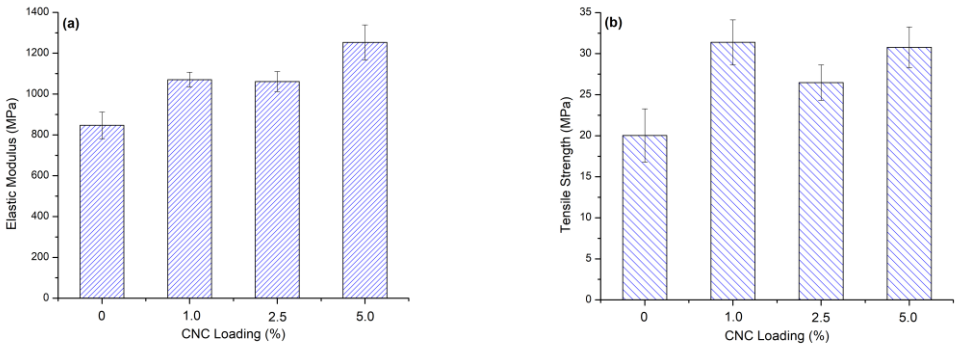

Figure 3. Mechanical properties of composites with different level of CNC loadings: elastic modulus (a) and tensile strength (b).

There is still increase in crystallinity of PA6 for 2.5%. Increase in agglomeration size and total amount of CNC can result in higher elastic modulus but relatively low tensile strength due to creation of imperfection or stress concentration in polymer. Increase in agglomeration size may prevent α phase formation due to some orientation and/or interaction differences compared to 1.0% and 2.5%. Although there are two ingredients in the system, agglomeration, size of agglomeration and distribution of agglomeration may play important role to stabilize crystals of PA6. Therefore, crystallinity of PA6, can give us clue about dispersion of PA6. When XRD, DSC and mechanical results are analysed, it can be concluded that highest distribution for1.0% CNC, moderate distribution with moderate agglomeration size for 2.5% CNC and moderate distribution with higher agglomeration size for 5.0% CNC are observed.

When mechanical and crystallinity results of pure PA6 and 1.0% CNC/PA6 are compared, it can be said that effect of CNC is higher than effect of crystallinity percent of PA6 on mechanical properties of composite. However, crystallinity percentage with crystal type which give vital information about dispersion of CNC, depending on spinning process. As spinning rate decreases, there might be more time for chains to be aligned and get interacted with CNC. In addition to physical experimental setup such as spinning rate, acceleration or solution preparation, another important parameter to increase dispersion or interaction between matrix and reinforcement is chemical modification of CNC. Although both CNC and PA6 are polar materials, grafting on CNC can help locking of chain movement of PA6. There has been a lot study on modification of CNC (Dufresne, Alain, 2013). Chemical modification of CNC and improvement of dispersion of it stays as a future work of this study.

4 CONCLUSION

This study examines reinforcement and nucleating effect of CNC on PA6 using solution based process. CNC reinforced PA6 composites are produced with spin coating process from formic acid, CNC and PA6 suspension. While there is no clear change in crystallinity percent of PA6, 48% and 54% increase in elastic modulus and tensile strength was observed, respectively. This study demonstrates promising results however it has not reached to its maximum value. Work is in progress to push further mechanical properties of CNC reinforced PA6 by changing spin coating process and modification of CNC.

5 ACKNOWLEDGEMENTS

The authors gratefully acknowledge the Alberta Innovates and Alberta-Ontario Innovation Program, FPInnovations (SFR02735 Nanocellulose Challenges) and Natural Science and Engineering Research Council of Canada (NSERC) Collaborative Research and Development Grants (CRDPJ 500602-16) for financial support.

REFERENCES

Dufresne, A. (2012). Nanocellulose: From nature to high performance tailored materials. *Nanocellulose: From nature to high performance tailored materials* (pp. 1-460) De Gruyter Mouton.

Dufresne, A. (2013). *Nanocellulose: A new ageless bionanomaterial* doi: https://doi.org/10.1016/j.mattod.2013.06.004

Fornes, T. D., & Paul, D. R. (2003). *Crystallization behavior of nylon 6 nanocomposites*. Polymer, 44(14), 3945-3961. doi:10.1016/S0032-3861(03)00344-6

Habr, J., Seidl, M., & Bobek, J. (2016). Impact of innovative cooling system on mechanical properties of moulded parts. *Defect and Diffusion Forum, 368*, 49-52. doi:10.4028/www.scientific.net/DDF.368.49

Kashani Rahimi, S., & Otaigbe, J. U. (2016). The role of particle surface functionality and microstructure development in isothermal and non-isothermal crystallization behavior of polyamide 6/cellulose nanocrystals nanocomposites. *Polymer, 107*, 316-331. doi:10.1016/j.polymer.2016.11.023

Kojima, Y., Usuki, A., Kawasumi, M., Okada, A., Fukushima, Y., Kurauchi, T., & Kamigaito, O. (1993). Mechanical properties of nylon 6-clay hybrid. *Journal of Materials Research, 8*(5), 1185-1189. doi:10.1557/JMR.1993.1185

Kuilla, T., Bhadra, S., Yao, D., Kim, N. H., Bose, S., & Lee, J. H. (2010). Recent advances in graphene based polymer composites. *Progress in Polymer Science (Oxford), 35*(11), 1350-1375. doi:10.1016/j.progpolymsci.2010.07.005

Lebaron, P. C., Wang, Z., & Pinnavaia, T. J. (1999). Polymer-layered silicate nanocomposites: An overview. *Applied Clay Science, 15*(1-2), 11-29. doi:10.1016/S0169-1317(99)00017-4

Liu, L., Qi, Z., & Zhu, X. (1999). Studies on nylon 6/clay nanocomposites by melt-intercalation process. *Journal of Applied Polymer Science, 71*(7), 1133-1138. doi:10.1002/(SICI)1097-4628(19990214)71:73.0.CO;2-N

Millot, C., Fillot, L., Lame, O., Sotta, P., & Seguela, R. (2015). Assessment of polyamide-6 crystallinity by DSC. *Journal of Thermal Analysis & Calorimetry, 122*(1), 307-314. doi:10.1007/s10973-015-4670-5

Murthy, N. S., Aharoni, S. M., & Szollosi, A. B. (1985). Stability of the γ form and the development of the α form in nylon 6. *Journal of Polymer Science: Polymer Physics Edition, 23*(12), 2549-2565. doi:10.1002/pol.1985.180231212

Nilagiri Balasubramanian, K. B., & Ramesh, T. (2018). Role, effect, and influences of micro and nano-fillers on various properties of polymer matrix composites for microelectronics: A review. *Polymers for Advanced Technologies, 29*(6), 1568-1585. doi:10.1002/pat.4280

Panthani, T. R., & Bates, F. S. (2015). Crystallization and mechanical properties of poly(l-lactide)-based rubbery/semicrystalline multiblock copolymers. *Macromolecules, 48*(13), 4529-4540. doi:10.1021/acs.macromol.5b01029

Paul, D. R., & Robeson, L. M. (2008). Polymer nanotechnology: Nanocomposites. *Polymer, 49*(15), 3187-3204. doi:10.1016/j.polymer.2008.04.017

Peitl, O., Oréfice, R. L., Hench, L. L., & Brennan, A. B. (2004). Effect of the crystallization of bioactive glass reinforcing agents on the mechanical properties of polymer composites. *Materials Science and Engineering A, 372*(1-2), 245-251. doi:10.1016/j.msea.2004.01.011

Qua, E. H., & Hornsby, P. R. (2011). Preparation and characterisation of nanocellulose reinforced polyamide-6. *Plastics, Rubber and Composites, 40*(6-7), 300-306. doi:10.1179/1743289810Y.0000000019

Shen, D., Fang, L., Chen, X., & Tang, Y. (2011). Structure and properties of polyacrylic acid modified hydroxyapatite/liquid crystal polymer composite. *Journal of Reinforced Plastics and Composites, 30*(13), 1155-1163. doi:10.1177/0731684411417318

Shishkovsky, I., Sherbakov, V., Ibatullin, I., Volchkov, V., & Volova, L. (2018). Nano-size ceramic reinforced 3D biopolymer scaffolds: Tribomechanical testing and stem cell activity. *Composite Structures, 202*, 651-659. doi:10.1016/j.compstruct.2018.03.062

Weng, W., Chen, G., & Wu, D. (2003). *Crystallization kinetics and melting behaviors of nylon 6/foliated graphite nanocomposites* doi:https://doi-org.login.ezproxy.library.ualberta.ca/10.1016/j.polymer.2003.10.028

Wunderlich, B. (1990). In Wunderlich B. (Ed.), *Thermal analysis* Academic Press. doi:https://doi-org.login.ezproxy.library.ualberta.ca/10.1016/B978-0-12-765605-2.50012-1 "

Ye, C., Wang, C., Wang, J., Wiener, C. G., Xia, X., Cheng, S. Z. D., Vogt, B. D. (2017). Rapid assessment of crystal orientation in semi-crystalline polymer films using rotational zone annealing and impact of orientation on mechanical properties. *Soft Matter, 13*(39), 7074-7084. doi:10.1039/c7sm01366c

Yousefian, H., & Rodrigue, D. (2017). Morphological, physical and mechanical properties of nanocrystalline cellulose filled nylon 6 foams. *Journal of Cellular Plastics, 53*(3), 253-271. doi:10.1177/0021955X16651241